Donald E. Davis

# Registration Mark Detection for Electron-Beam Lithography—EL1 System

*In electron-beam lithography for the direct exposure of wafers for integrated circuit manufacturing, accurate registration is necessary to achieve the required pattern overlay. This paper examines elements that should be considered to optimize the registration mark detection process in an automatic registration system for an e-beam lithography tool such as IBM's EL1. Included is a section on the generation of the backscatter signals and the proper combination of these signals to reduce the detection uncertainty errors in a system with four backscatter detectors. Signals obtained from resist-coated marks with several vertical profiles are presented for illustration and comparison with the predicted results. Beam shot noise, resist effects, and other factors that affect the signal-to-noise ratio are discussed and some pattern overlay results from EL1 are given.*

## Introduction

Electron-beam lithography tools [1-5] are maturing and today are found not only in the laboratories but also on the manufacturing floors of semiconductor fabricators. The success of e-beam lithography rests on three pillars, namely the attainment of high resolution, high throughput, and accurate overlay, *i.e.*, the matching of patterns in multi-level lithography. E-beam lithography has demonstrated the resolution [6] required to write submicron images (electron optics is not diffraction-limited at these dimensions as is light optics). The use of the shaped spot and other features such as autoregistration and automatic wafer (or mask) handling [7] have made it possible to write today's circuit product patterns reliably at the throughputs required for economical production [8]. Variable shaped-spot tools [9] will further increase this throughput. The direct exposure of wafers requires the capability of the exposure tool to accurately match the pattern to be exposed to the processed pattern already on the wafer. Since the pattern exposure in the scanning-type e-beam tools uses deflection of the beam, accurate pattern overlay is possible by simply applying on-the-fly corrections to the deflection signals. These corrections are based on the data provided by automatic registration. Many e-beam tools employ the technique of four-corner registration [10-12] to provide translation, rotation, magnification, and trapezoidal corrections at each chip site.

The registration process includes scanning the e-beam across registration marks on the workpiece and observing the resultant backscattered signals to determine the relative positions of the e-beam and the patterns already on the workpiece. This paper discusses this process for the IBM EL1 e-beam lithography tool [7] in particular and some considerations for obtaining an optimal detection system in general.

## Backscattered electrons and detectors

In a typical e-beam lithography tool, electrons strike the workpiece with 25 keV of energy. (1 keV = 1.602 $\times 10^{-16}$ J. Throughout the text energy values are given in keV.) These electrons penetrate the workpiece and collide with the atoms of the material. The registration process is performed on registration marks covered by 0.5 to 3.5 $\mu$m of e-beam-sensitive resist. Some primary electrons that experience elastic and/or inelastic collisions and have been modulated by the registration marks are backscattered and escape the surface. The collisions will also produce secondary electrons (<100 eV energy). Only the secondary electrons generated near the surface have enough energy to escape the target. These secondary electrons may be generated by incoming electrons and contain information only about the surface of the resist, or they may be generated by the modulated backscattered

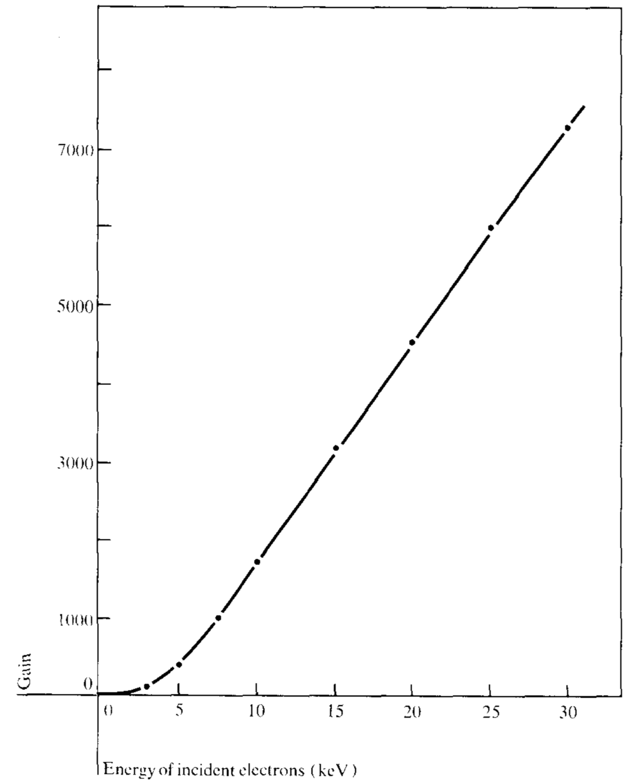


**Figure 1** Diode detector current gain *vs* energy of incident electrons. Gain equals detector current out divided by incident current on detector.

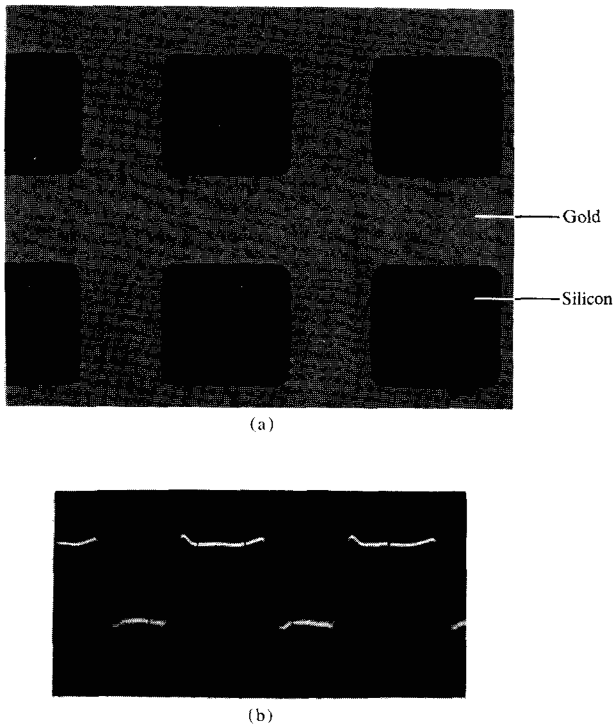


**Figure 2** Backscatter signals generated from material differences on the target: (a) calibration grid; (b) analog signal from grid.

primary electrons from within the material and also contain some information about the underlying registration mark.

Channel multipliers, scintillators [13], and diffused junction diode detectors are some of the devices used to sense the backscattered electrons. In the EL1 and EL2 [9] lithography tools, diffused junction diode detectors are used. These backscattered electron detectors are more suitable for sensing registration marks beneath thick coatings of resist than are secondary detectors. Also, the predictable and stable gain characteristics of the diode detectors are desirable for detectors used in a completely automatic registration system than channel multipliers or scintillators. There are four detectors mounted orthogonally to one another and 4 mm above the workpiece surface. The solid angle subtended by each diode detector is 0.43 steradian. These diodes have guard rings to reduce the dark current to below 0.2 $\mu$A and are biased to operate fully depleted with the junctions turned away from the electron impact area. These detector diodes are sensitive to the energy of the incoming electrons, producing a hole-electron pair for each 3.8 eV of ionizing potential. Thus, each backscattered electron striking this detector with 25 keV of energy produces approximately 6000 hole-electron pairs which are swept out of the depletion region as output current. The detectors have a linear response except for a loss of gain (Fig. 1) for low-energy incident electrons caused by a small "dead band" of higher-conductivity material which prevents the depletion layer from extending to the front surface.

## Signal generation

As the beam is swept across a registration mark, the backscattered electrons are modulated and signals are generated. This modulation process can be thought of as two distinct phenomena: modulation as the beam crosses from one material to another and modulation as the beam crosses a step or contour.

- *Backscattered signals generated from material differences*

When an electron beam impinges upon a solid target, some of the electrons are scattered back toward the source. The backscattering coefficient (or backscattered fraction) is the ratio of the number of electrons backscattered from the target to the number of electrons striking the target. Holiday and Sternglass [14] demonstrated that in the keV range and above this coefficient is an atomic characteristic independent of the crystal structure or the conduction properties of the solid. Archard [15] plots the backscattered coefficient *vs* the atomic number obtained from experimental data points from various researchers. In general, the greater the atomic number of a material, the greater is its backscattering coefficient. Scanning an electron beam across a target composed of two materials produces a change in the number of backscattered electrons as the beam crosses from one material to the next. For example, in the EL1 system there is a calibration grid composed of 1-$\mu$m-thick mesh of gold ($Z = 79$) on a silicon ($Z = 14$) substrate. The electron beam is scanned across this grid and the resultant backscattered signals are used to determine corrections that are applied to linearize the deflection [16]. A section of this grid and the high-contrast backscattered signal (the sum of four detectors) are shown in Fig. 2; the signal is due almost entirely to the material differences of the target.

It has been shown [11, 17] that gold or other materials with high atomic numbers can be used in forming the registration marks to enhance the backscattered signal from these marks. Unfortunately, the extra process steps required in fabrication and the possible contamination of semiconductor devices make this approach undesirable.

• *Backscatter signals generated from contours or edges*
When an electron beam is scanned across an edge or step in the surface of a homogenous material, a signal is generated. Figure 3 can be used to illustrate the means by which this signal is produced. The electrons from the beam penetrate beneath the surface of the target, experience collisions, and are backscattered toward the detectors X1 and X2. The backscattered electrons are modulated by the steps or contours on the surface or within the target. In this figure, for example, the signal to detector X2 is stronger than that to detector X1 because of the decreased path length within the target back to detector X2.

A simple backscatter model predicts the actual signal shapes to a first approximation. The model assumes that only a single collision occurs at a depth equal to one-half the range of the electrons into the material and derives the signal modulation from the path length that the backscattered electrons traverse in the target. The signals predicted by such a model for two detectors X1 and X2, placed orthogonally to the beam scanning direction, are shown in Fig. 3. For comparison, Fig. 4 shows photographs of signals from four orthogonally placed detector diodes (X1, X2, Y1, Y2) as a 2.5-$\mu$m-square beam is swept in the $X$ axis across a single-bar registration mark located in the corner of a 5-mm field. The mark was formed by etching through a 0.5-$\mu$m $SiO_2$ layer to a Si substrate and was coated with 2.0 $\mu$m of resist. Each edge crossing produces a slow (shallow) and fast (steep) transition in the signal modulation. The slow transition is produced as the beam approaches or recedes from the edge; the fast transition is produced just as the beam crosses the mark edge and the average collision depth changes.

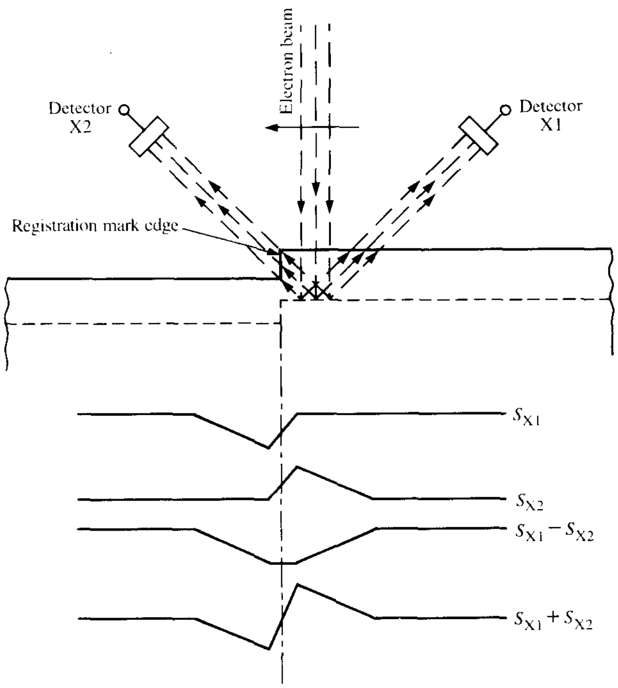


**Figure 3** Backscatter signals generated from contours on the target.

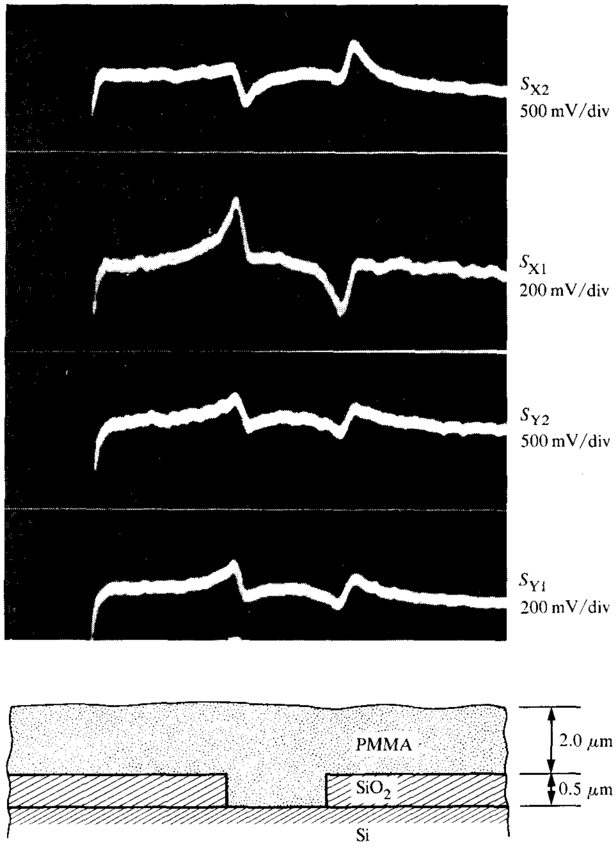


**Figure 4** Individual detector signals generated from a 25-$\mu$m-wide single-bar registration mark.

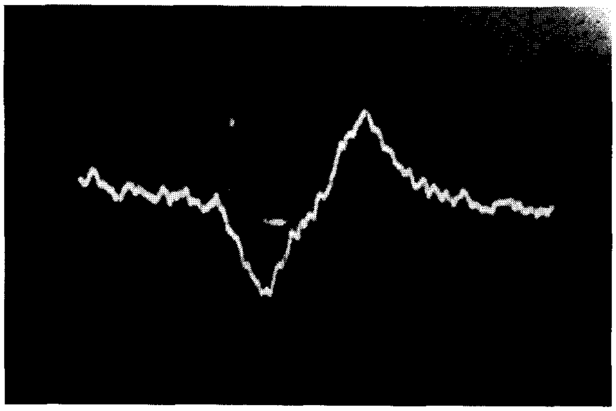

(a)

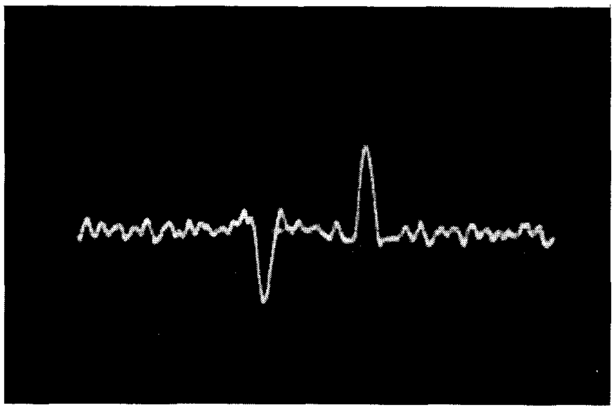

(b)

**Figure 5** Registration signal improvement by using differential of sum rather than difference signal processing. Registration mark depth equals 0.7 $\mu$m and resist thickness equals 2.5 $\mu$m. (a) the difference signal $S_{X1} - S_{X2}$; (b) the derivative of the sum signal $d/dt(S_{X1} + S_{X2} + S_{Y1} + S_{Y2})$. In both plots the vertical scale is 200 mV/cm and the horizontal scale is 20 $\mu$s/cm.

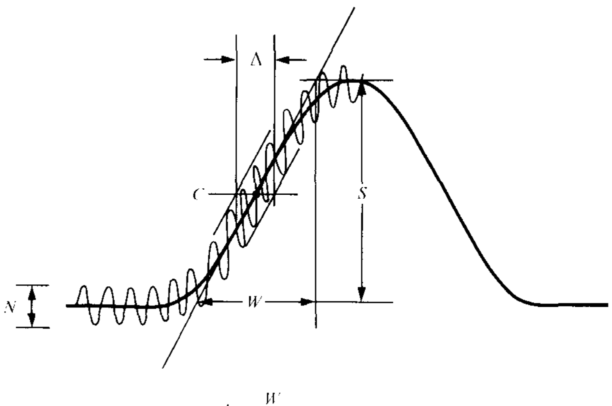


$$\Delta = \frac{W}{S/N}$$

**Figure 6** Detection uncertainty $\Delta$.

The width of the fast transition is produced by the finite width of the beam convoluted with the edge slope of the mark. Due to electron scattering, the beam width increases as it penetrates into the sample, causing this transition to be wider on samples coated with thick resist. It has been found, however, that the fast transitions are much less affected by thick coatings of resist than are the slow transitions.

Figure 3 represents waveforms obtained by assuming a beam with a square cross section with an edge slope small compared to the beam width. An increase in the edge slope would result in a rounding of the corners of the waveforms in this figure. A round SEM-type electron probe with a Gaussian profile would result in both rounded corners of these waveforms and transitions that were nonlinear to correspond to the nonlinear beam cross section being swept across the edge.

If the signals are subtracted ($S_{X1} - S_{X2}$), a signal is produced that eliminates the fast transition. If the signals are added ($S_{X1} + S_{X2}$), a signal is produced in which this fast transition is reinforced (see Fig. 3).

Stephani [18] has used a Monte Carlo model given by Kyser and Murata to simulate image formation by backscattered electrons from registration marks formed by steps in silicon. The primary electron beam was assumed to have a Gaussian distribution with a narrow width [FWHM (full width half magnitude)] of 0.1 $\mu$m. The results obtained by using this model show a very sharp transition at the mark edge and lead to the conclusion that the sum signal is superior to the difference signal. If the sum signal is differentiated [19], a signal is produced whose amplitude is proportional to the width of the fast transition and whose peaks approximately correspond to the position of the beam as it crosses the mark edges. Comparing this signal with the simple difference signal from two diodes ($S_{X1} - S_{X2}$) would reveal a peaked signal in both cases, but with the differentiated signal having the narrower width. Figure 5 shows two such signals (the differentiated signal includes the signals from all four detectors) obtained by scanning a 2.5-$\mu$m-square beam across a single bar etched 0.7 $\mu$m through $Si_3N_4$ and $SiO_2$ layers above a Si substrate and coated with 2.5 $\mu$m of resist. Note that both signals have approximately the same peak signal amplitude and noise amplitude but that the differentiated signal is narrower. To illustrate that a narrow signal is preferred, refer to Fig. 6, which depicts a signal with amplitude $S$ with a superimposed random noise background of amplitude $N$. If this signal is threshold-detected at point $C$, the detection uncertainty $\Delta$ is directly proportional to $W$, a measure of the signal width. A narrower signal will have a smaller $W$ with a correspondingly smaller detection uncertainty. By repeated scans across the marks and by using marks with multiple edges the random error in locating the registration marks can be further reduced:

$$\text{Error} = \frac{W}{(S/N)\sqrt{(\text{no. of edges}) \times (\text{no. of scans})}}.$$

Figure 7 plots this theoretical detection uncertainty of locating the registration mark *vs* the signal-to-noise ($S/N$) ratio resulting from a single scan for the conditions $W$ = 4 $\mu$m; no. edges = 2, 4; no. scans = 30. This applies to a registration system that uses simple threshold detection.

The $S/N$ ratio can be improved before threshold detection by scanning the mark repeatedly and averaging [11] the result of each scan line. The averaging process reduces random noise components by the square root of the number of scans. Also, correlated noise components that occur only on some scan lines may be reduced below the threshold for signal detection, but completely correlated noise cannot be reduced by this technique. Signal averaging before threshold detection is particularly useful for improving low $S/N$ ratios to the point where reliable threshold detection can be accomplished. Signal averaging also results in the reduction of data one has to process.

If the $S/N$ ratio is high enough, threshold detection can be done on each scan and the mark location determined by averaging the results from all scans by software. Most of the random and correlated noise pulses above the threshold can be edited from each scan by comparing the data to an expected sequence of signal data points obtained from a model of the registration mark. A detailed explanation of such an algorithm is contained in Reference [10] and need not be repeated here.

Reference [20] describes a third type of signal processing that combines signal averaging and moment calculations. Rather than relying only on the threshold points to determine the mark locations, the moment calculations utilize many data points above each threshold. This technique should further reduce the error due to random noise components.

Because changes in time delays in the detection channel may be misinterpreted as mark position changes, it is desirable to scan the registration marks in both directions, forward and backward, to cancel these delays. The edges of registration marks vary widely in their slope, depth, and composition and they may be covered with different materials. This wide variety of edges will produce backscatter signals with different shapes and peak

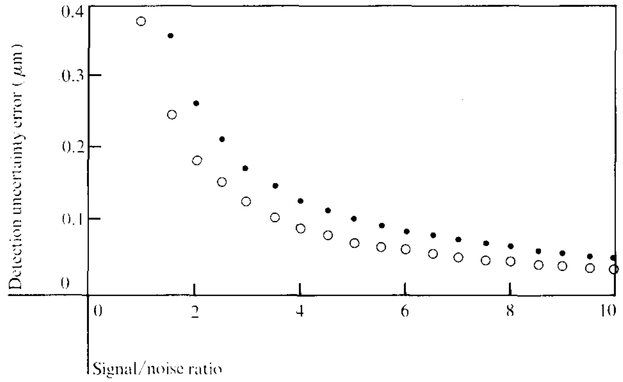


**Figure 7** Detection uncertainty error (signal width $W$ = 4 $\mu$m, 30 scans across the mark) *vs* signal-to-noise ratio; ●, mark with two edges. ○, mark with four edges.

locations relative to the different edges. For this reason, edges of registration marks are treated as pairs to determine the mark centerline. This centerline is used to define the mark location to avoid the problem of correlating the backscatter signal peaks to single edges. Also, the mark centerline does not move if the registration mark width varies as a result of under- or over-etching during wafer processing. In Fig. 8 are photographs of oscilloscope traces of the backscatter signals from a two-bar mark 2.3 $\mu$m deep, coated with 3.2 $\mu$m of resist. Here again the differentiated sum signal has produced sharp peaks corresponding to the mark edges when it is compared to the difference signal produced by subtracting the detector signals. The sum signal and the differential signal also reveal another phenomenon, the enhancement effect [21], which produces a reinforcement of the signals from edges that are placed an optimum distance apart for a given set of conditions. In Fig. 8 this results in a somewhat larger signal amplitude produced by the two inner edges of the registration mark as compared to the outside edges. In practice, although the registration marks are usually reused at different levels of the device processing and it is not possible to optimize exactly the mark widths and spacings for all of the resultant cases of mark depths and resist thicknesses, the registration mark design can be optimized for the most critical overlay level.

Typically, the backscatter signal obtained by scanning registration marks is a superposition of signals generated from both material differences and from contours or edges. An understanding of these two basic processes allows one to predict the backscatter signal amplitudes and shapes from a wide variety of registration marks.

### Signal-to-noise ratio

Certain electrical noise sources must be considered in the determination of the available signal-to-noise ratio in a

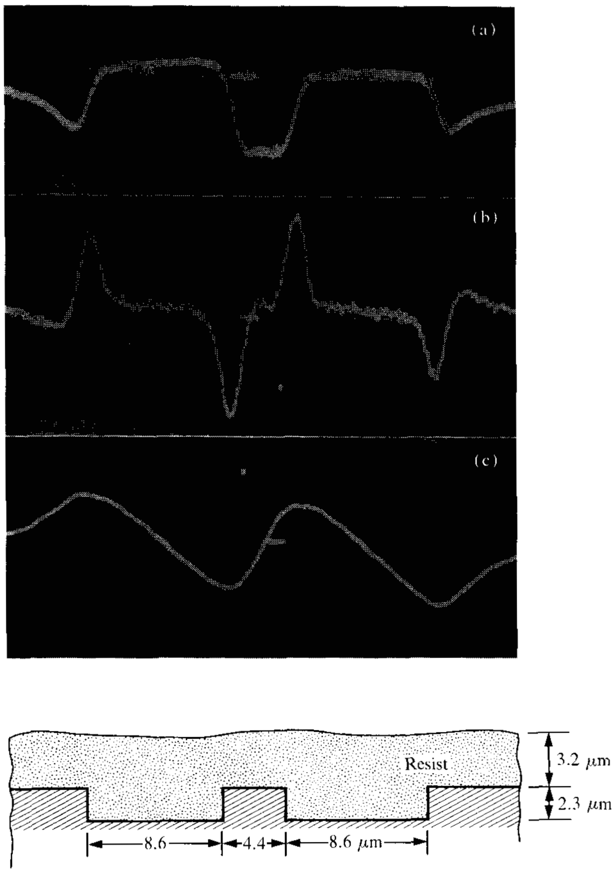


**Figure 8** Backscatter signals from a two-bar registration mark coated with thick resist: (a) $S_{X1} + S_{X2} + S_{Y1} + S_{Y2}$; (b) $(d/dt)(S_{X1} + S_{X2} + S_{Y1} + S_{Y2})$; (c) $S_{X1} - S_{X2}$.

detection system. A primary noise source is the shot noise of the e-beam itself. The shot noise arises from the random emission of electrons from the e-gun cathode. This causes the beam current to be not smooth and continuous but a summation of discrete changes. This variation in this flow is the shot noise, and the rms value can be determined from the equation

$$I_n^2 = 2eIB_n$$

(see Reference [22]), where $I_n$ = noise current, $e$ = electronic charge, $I$ = current, and $B_n$ = bandwidth of the system. That portion of the backscattered beam current intercepted by a detector is $I_2/G$, where $G$ is the detector current gain and $I_2$ is the detector output current. Therefore, the noise current into the detector is

$$I_{n_1} = \sqrt{2e \frac{I_2}{G} B_n}.$$

The output noise current from each detector is

$$I_{n_2} = GI_{n_1} = \sqrt{2eI_2GB_n}.$$

For the EL1 system, typical values are $I_2$ = 100 μA (background current, Si wafer target), $G$ = 6000 (assumes all elastic collisions), and $B_n$ = 250 kHz, resulting in an output noise current $I_{n_2}$ = 0.22 μA.

This calculated shot noise has been verified by measuring the noise from the detector diodes while the beam is stationary on the target. Experiments have also verified that while the signal is directly proportional to that portion of the backscattered beam current intercepted by a detector, the rms noise is proportional to the square root of this current, as predicted by these equations. Therefore, the $S/N$ ratio will be improved as the beam current is increased in a system. The backscatter signal should be maximized by locating large detectors near the target. The bandwidth of the system should be no larger than necessary to pass the signal without distortion. A higher acceleration potential in the e-beam column will result in higher-energy backscattered electrons which will also produce a better $S/N$ ratio.

For a system with a large beam current (3 μA) such as EL1, the detector current output current can be amplified using a low-noise operational amplifier in the transimpedance mode with a noise contribution from the amplifier that is negligible. Thermal noise from associated resistors is also negligible. Although there is shot noise generated in the detectors, it is small compared to shot noise generated by the electron beam itself, which remains a primary noise source for the system. Surface roughness of the workpiece also produces noise as the beam is scanned across the registration marks.

## Registration marks

Registration marks must be compatible with the manufacturing processes. The initial marks could be etched holes [23], etched V-grooves [24], or more usually etched steps or raised bars in $SiO_2$ or Si. These initial marks typically must survive subsequent processing steps, and the resultant marks may consist of several layers of different materials.

At each patterning step in the fabrication process, the choice must be made as to the registration mark for the next patterning step. A new mark may be written along with the present pattern to be used at the next step, or the old registration mark may be used again if it has not deteriorated. In general, it is desirable to reuse registration marks, where possible, as each new mark written will have an additional positioning error compared to the original mark.

## Resist effects

The registration marks must be sensed through a coating of e-beam resist such as poly-methyl-methacrylate (PMMA). The resist covers the complete target that is about to be exposed. The resist could be selectively exposed, developed, and removed from the area of the registration marks prior to the registration process, but because of the extra processing steps required this is rarely done.

The thickness of the resist coating directly affects the backscattered signal amplitude from an underlying registration mark. Figure 9 plots PMMA resist thickness *vs* the backscatter signal received by one detector diode from a registration mark. The mark was formed by etching through a 0.7-$\mu$m $SiO_2$ layer on a Si substrate.

When scanning the registration marks, the e-beam radiation induces physical and/or chemical changes within the resist, producing scissions or cross-linking of these organic polymers. Local heating occurs and there may be gases released within the resists. The combination of high beam intensity, slow scanning speed, and thick coatings of resist may cause the decomposition to occur too rapidly with a resultant burning or bubbling of the resists. The bubbling resist distorts the backscattered signals from the underlying registration marks. This distortion appears as correlated noise and will obscure or shift the registration mark signal.

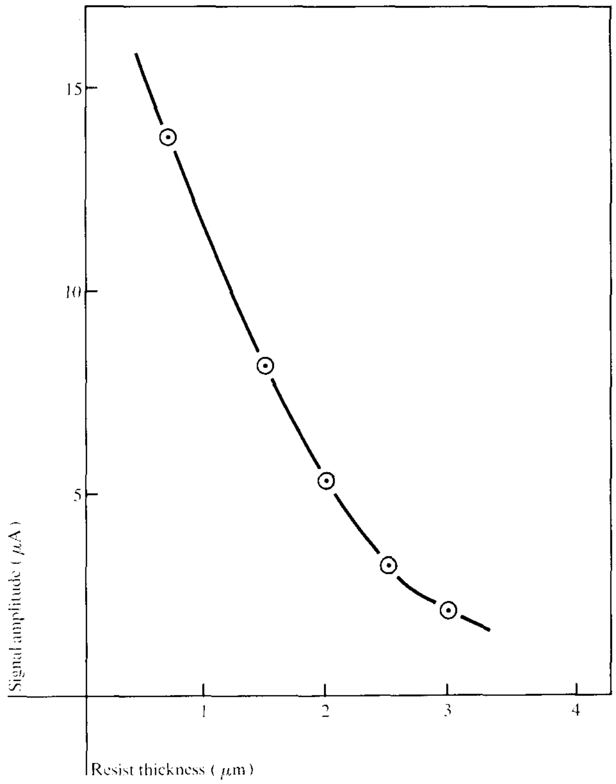


**Figure 9** Registration backscattered signal amplitude *vs* resist thickness. Resist type is PMMA. Mark depth = 0.7 $\mu$m.

To prevent bubbling, the e-beam spot can be effectively elongated in a direction orthogonal to the scanning direction by superimposing a "dither" motion on the registration scans. In the EL1 system, a $\pm$22.5-$\mu$m triangular 10-mHz orthogonal motion is superimposed on a registration scanning speed of 1.6 $\mu$m/$\mu$s. The dither motion is transparent to the registration operation, but does disperse the energy of the beam over a larger area, reducing the peak temperature of the area being scanned. This allows three sets of 30 scan lines to occur over a resist thickness of up to 3.5 $\mu$m without bubbling. The spot size for these scans is approximately 6 $\mu m^2$ with a beam current density of 50 $A/cm^2$.

Figure 10 shows photographs of the backscattered signals for 15 scans: (a) over a single-bar mark (with dither), (b) over a resist-coated flat area on a wafer (with dither), and (c) over a resist-coated flat area on a wafer (without dither) showing the dynamic formation of bubbles.

## Results

The ultimate test for a registration detection system is the ability of the lithography tool using the registration system to produce good pattern overlays. However, the registration detection errors are only one of many system error components that must be kept to a minimum as they combine to make up the total overlay error.

Figure 11 is a plot of the overlay errors between two patterns on a wafer. The first pattern (including registration marks in each corner) was first written at each of 86 chip sites on the wafer. The wafer was developed, etched, and recoated with resist and the second pattern was registered and written at each chip site. The wafer was again developed and etched and the overlay errors in both $X$ and $Y$ between these two patterns were measured in each of the four corners of all 86 sites. The overlay error is generally worse in the corners than near the centers of the chips. The mean value and the $3\sigma$ value of these errors are given in Table 1. These data show a systematic error in the means of the overlay errors that could be largely calibrated out of the system; however, the system was performing well within the overlay specification of 0.75 $\mu$m at this time. More importantly, the data show a $3\sigma$ random component of these overlay errors that is less

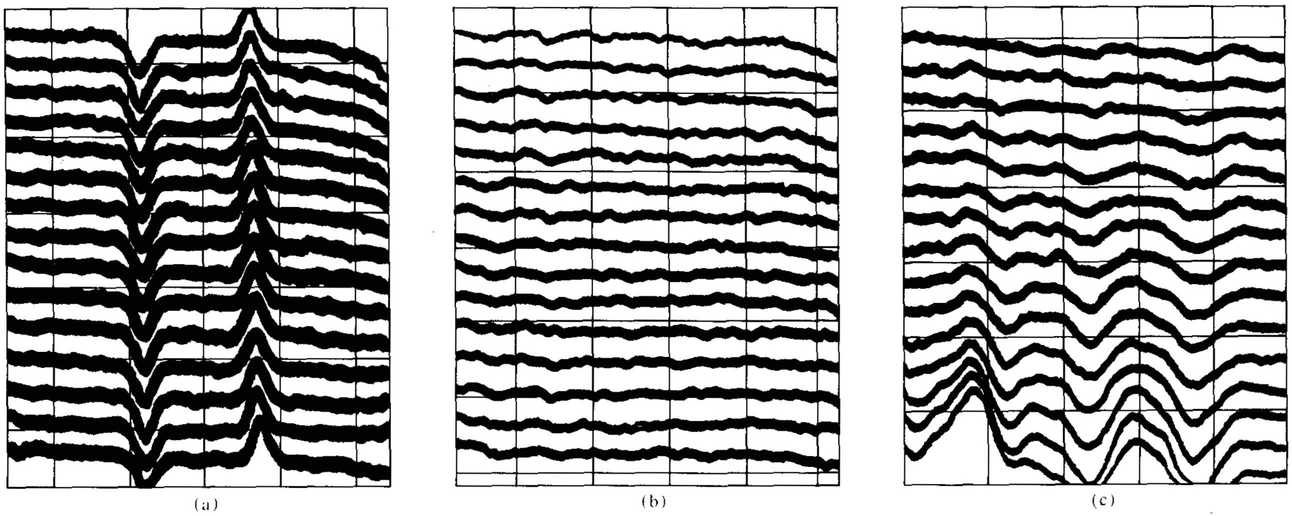


**Figure 10** Backscattered signals from a resist-coated wafer showing bubble generation (15 scans): (a) Single-bar mark with deflection dither; (b) flat wafer surface with deflection dither resulting in no bubble generation; and (c) flat wafer surface without deflection dither resulting in bubble generation.

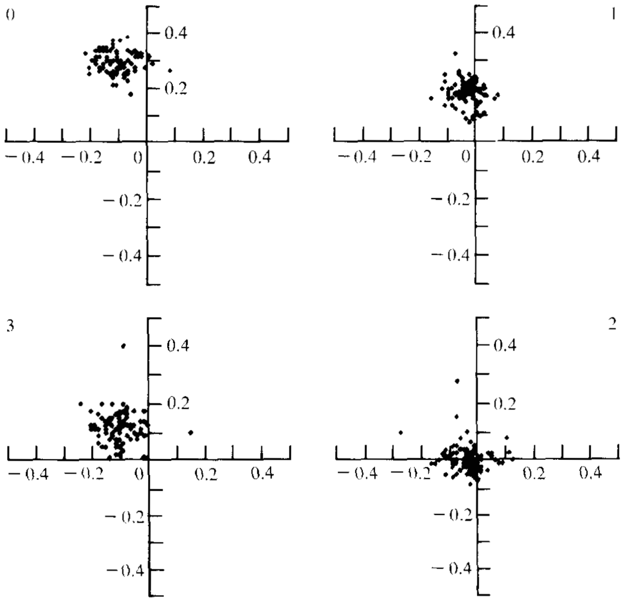


**Figure 11** EL1 pattern overlay errors plotted by corner ($\mu$m). Mark height = 0.5 $\mu$m. Resist thickness = 1.5 $\mu$m. Results for 86 chips of size 5 × 5 mm.

than 0.2 $\mu$m. This random component of the overlay error is due to several sources, including beam jitter, random magnetic deflection errors, registration correction errors, and registration detection errors. It is estimated that the registration detection component of this overlay error is less than 0.1 $\mu$m. This overlay was done using the EL1 system [7, 10] with the following parameters:

| | |
|---|---|
| registration mark type | 2-bar, recessed |
| registration mark depth | 0.5 $\mu$m |
| resist thickness, type | 1.5 $\mu$m, PMMA |
| detection bandwidth | 250 kHz |
| registration scanning speed | 1.6 $\mu$m/$\mu$s |
| number of scans | 15 forward, 15 reverse |
| chip size | 5 mm × 5 mm |
| beam size | 2.5 $\mu$m × 2.5 $\mu$m |
| beam current | 3 $\mu$A |
| accelerating potential | 25 kV |

These data are an example of the capability of the EL1 system to perform pattern overlays using a detection system that has been optimized for registrations on marks covered with thick resist coatings.

**Table 1** Summary of EL1 overlay errors in Fig. 11 in units of $\mu$m.

| | *X0* | *X1* | *X2* | *X3* | *Y0* | *Y1* | *Y2* | *Y3* |
|---|---|---|---|---|---|---|---|---|
| Mean | −0.11 | −0.03 | −0.03 | −0.09 | 0.29 | 0.19 | 0.01 | 0.12 |
| $3\sigma$ | 0.16 | 0.13 | 0.19 | 0.17 | 0.12 | 0.13 | 0.15 | 0.16 |

## Summary

Fundamental considerations for detecting registration marks in the EL1 system and other e-beam lithography tools have been examined. Backscattered signal components have been separated into two components, those generated from material differences and those generated from contours on the target. A simple model has been given that approximates the signals produced by the latter. It has been shown that for thick coatings of resist, using the sum of the registration signals from the detectors results in a smaller detection error than that obtained by using the difference signals. Finally, some thick resist pattern overlay results from EL1 have been presented.



## Acknowledgments

The author is indebted to many members of the EL1 and EL2 design teams. In particular, contributions by E. V. Weber, O. C. Woodard, M. H. Habegger, M. C. Williams, and W. Stickel have been most helpful and are appreciated.


## References


1. E. V. Weber and R. D. Moore, "E-Beam Exposure for Semiconductor Device Lithography," *Solid State Technol.* **22,** 61 (1979).
2. D. R. Herriott, R. J. Collier, D. S. Alles, and J. W. Stafford, "EBES: A Practical Electron Lithographic System," *IEEE Trans. Electron Devices* **ED-22,** 385 (1975).
3. G. L. Varnell, R. A. Williamson, T. L. Brewer, J. L. Bartelt, R. J. Dexter, R. A. Robbins, and C. D. Winborn, "IC Fabrication Using Electron-Beam Technology," *First Quarterly Report, Contract #DAA307-76-C-8105*, U.S. Army Electronics Command, Fort Monmouth, NJ, January 1977.
4. R. A. Geshner, "The Electron Beam: A Better Way to Make Semiconductor Masks," *RCA Engineer* **24,** 47 (1978).
5. S. Miyauchi, "Electron-Beam Exposure Systems Provide Better Quality Masks Faster," *J. Electrical Engineer* (Denpa Publications, Tokyo, Japan) **35,** 60 (1978).
6. T. H. P. Chang, M. Hatzakis, A. D. Wilson, and A. N. Broers, "Electron-beam lithography draws a finer line," *Electronics* **50,** 89 (1977).
7. H. S. Yourke and E. V. Weber, "A High-Throughput Scanning-Electron-Beam Lithography System, EL1, for Semiconductor Manufacture: General Description," *IEDM Tech. Digest*, 431 (1976).
8. N. G. Wu, "Automated Wafer Production," *Proceedings of the IEEE International Solid State Circuits Conference*, San Francisco, CA, February 1980.
9. E. V. Weber and R. D. Moore, "Variable Spot-Shaped E-beam Lithographic Tool," *J. Vac. Sci. Technol.* **16,** 1780 (1979).
10. D. E. Davis, R. D. Moore, M. C. Williams, and O. C. Woodard, "Automatic Registration in an Electron-Beam Lithographic System," *IBM J. Res. Develop.* **21,** 498 (1977).
11. A. D. Wilson, T. H. P. Chang, and A. Kern, "Experimental Scanning Electron-Beam Automatic Registration System," *J. Vac. Sci. Technol.* **12,** 1240 (1975).
12. N. Saitou, C. Munakata, Y. Miura, and Y. Honda, "Computer-Controlled Electron-Beam Microfabrication Machine with a New Registration System," *J. Phys. E* **7,** 441 (1974).
13. T. H. P. Chang, "Detection of Electronic Signals for Microfabrication Registration," *Proceedings of the Eighth International Congress on Electron Microscopy* (Australian Academy of Sciences, Canberra) **I,** 650 (1974).
14. J. E. Holliday and E. J. Sternglass, "Backscattering of 5-20 keV Electrons from Insulators and Metals," *J. Appl. Phys.* **28,** 1189 (1957).
15. G. D. Archard, "Back Scattering of Electrons," *J. Appl. Phys.* **32,** 1505 (1961).
16. H. Engelke, J. F. Loughran, M. S. Michail, and P. M. Ryan, "Correction of Nonlinear Deflection Distortion in a Direct Exposure Electron-Beam System," *IBM J. Res. Develop.* **21,** 506 (1977).
17. E. D. Wolf, P. J. Coane, and F. S. Ozdemir, "Composition and Detection of Alignment Marks for Electron-Beam Lithography," *J. Vac. Sci. Technol.* **12,** 1266 (1975).
18. D. Stephani, "Monte Carlo Calculations of Back Scattered Electrons at Registration Marks," *J. Vac. Sci. Technol.* **16,** 1739 (1979).
19. D. E. Davis, M. A. Habegger, and H. S. Yourke, "Apparatus for Detecting Registration Marks on a Target Such as a Semiconductor Wafer," U.S. Patent 4,056,730, November 1, 1977.
20. D. E. Davis, R. D. Jackson, M. C. Williams, and O. C. Woodard, "Hardware Technique for Processing Electron-Beam Backscatter Signal for Registration," *IBM Tech. Disclosure Bull.* **22,** 140 (1979).
21. W. Stickel, "Method of Optimizing Registration Signals for Electron-Beam Microfabrication," *J. Vac. Sci. Technol.* **15,** 901 (1978).
22. M. I. Skolnik, *Introduction to Radar Systems*, McGraw-Hill Book Co., Inc., New York, 1962, p. 362.
23. Y. Lida and T. E. Everhart, "High Contrast Registration Marks for Electron-beam Pattern Exposure on (100) Silicon," *J. Vac. Sci. Technol.* **15,** 917 (1978).
24. H. Friedrich, H. U. Zeitler, and H. Bierhenke, "Optimization of Alignment Marks and Their Electron Signals in a Semiconductor Process," *Proceedings of the Seventh International Conference on Electron and Ion Beam Science and Technology*, Washington, DC, May 1976; R. Bakish, Ed., The Electrochemical Society, Princeton, NJ, 1976, p. 340.



*Received March 25, 1980; revised April 29, 1980*



*The author is located at the IBM Data Systems Division laboratory, East Fishkill (Hopewell Junction), New York 12533.*